Food & Medicine Homology

ISSN 3006-6867 (print); 3006-4252 (online)
https://doi.org/10.26599/FMH.2024.9420008

Research Article

Artemisia argyi polysaccharide alleviates intestinal inflammation and intestinal flora dysbiosis in lipopolysaccharide-treated mice

Er-Juan Ning[1,2], Chao-Wei Sun[2], Xue-Fang Wang[1,2], Ling Chen[1,2], Fei-Fei Li[1,2], Li-Xian Zhang[1,2], Lu-Peng Wang[1,2], Yan-Ni Ma[1,2], Jie Zhu[1,2], Xiao Li[1,2] (✉), Wei Wang[1,2] (✉)

[1] *Henan Natural Products Biotechnology Co., Ltd., Zhengzhou 450002, China*
[2] *Henan Academy of Sciences, Zhengzhou 450002, China*

Received: 29 March 2024 / **Revised:** 17 May 2024 / **Accepted:** 21 May 2024

Abstract: *Artemisia argyi* polysaccharide (AAP) is an important active component extracted from the leaves of *A. argyi*. Currently, the effects of AAP in mouse model of intestinal inflammation are unclear. At the same time, it is uncertain whether AAP affects the intestinal flora. The study aimed to explore the improvement effects of AAP on lipopolysaccharide (LPS)-treated mice. The changes of intestinal tissue was observed with hematoxylin-eosin (HE) staining, also the mRNA expression of the intestinal barrier-related junction proteins were detected. The intestinal oxidation indices and inflammatory factors were detected with ELISA method, the nuclear factor kappa B (NF-κB) signaling pathway expression was evaluated with Western blotting, and the contents of short-chain fatty acids (SCFAs) in the colon were determined. At the same time, the changes of AAP on intestinal flora were evaluated. The study have shown that AAP downregulated the expression of NF-κB inhibitor protein α (IκBα), improved intestinal stress state, and inhibited the production of tumor necrosis factor-α (TNF-α), interleukin-6 (IL-6), interleukin-17 (IL-17), and interleukin-1β (IL-1β) in intestinal tissues. The contents of SCFAs (acetic acid, propionic acid, butyric acid) in the colon were increased, the numbers and composition of intestinal flora were changed after AAP intervention. In conclusion: AAP alleviated intestinal inflammation and intestinal flora dysbiosis in LPS-treated mice, it may play a key role in maintaining the intestinal barrier by regulating intestinal flora.

Keywords: *Artemisia argyi* polysaccharides; intestinal inflammation; intestinal barrier; intestinal flora; NF-κB signaling pathway

Citation: Ning E. J., Sun C. W., Wang X. F., et al. *Artemisia argyi* polysaccharide alleviates intestinal inflammation and intestinal flora dysbiosis in lipopolysaccharide-treated mice. *Food & Medicine Homology*, 2024, 1: 9420008. https://doi.org/10.26599/FMH.2024.9420008

1 Introduction

With the changes of people's diet (the intake of high-fat, high-sugar diet, irregular diet), chaotic work, decreased rest time and increase of life pressure; the incidence of intestinal inflammatory diseases has gradually increased in recent years, leading a serious threat to human health[1]. The intestine is the main organ for digestion and absorption of nutrients. As a selective barrier, the intestinal mucosa constitutes the main component of human immunity and is the largest immune organ. Intestinal mucosa is enriched with blood vessels, and inflammation can lead to damage to the barrier. Intestinal barrier damage also causes intestinal inflammatory diseases and bacterial enteritis[2]. At present, the treatment of intestinal inflammation mainly relies on antibiotics. Although the therapeutic effects are obvious, several clinical complications such as antibiotic resistance, antibiotic-associated diarrhea, repeated infections, and intestinal flora-associated metabolic disorders may occur. A lot of evidence shows that some bioactive compounds consist in food play an improtant role in intestinal inflammation by affecting inflammatory mediators, barrier integrity, and intestinal flora composition[3,4]. Therefore, natural compounds without side effects on intestinal could effectively prevent or reduce intestinal inflammation, reduce intestinal mucosal damage, and regulate intestinal flora balance; so it can be used as a new way to treat intestinal inflammatory diseases.

Artemisia argyi is a perennial herbaceous plant widely distributed in China. *A. argyi* leaf is a famous traditional Chinese medicine and edible resource, which has a history of more than 3,000 years in China, Korea, Japan, and other countries[5,6]. The fresh leaves are often used to cook porridge or make glutinous rice balls in China. Polysaccharide extrated from *A. argyi* is an important active ingredient that has immune-enhancing, antitumor, anti-inflammatory, antiviral, and antioxidant activities among others[7,8]. As a carbohydrate macromolecule, *A. argyi* polysaccharide (AAP) cannot be directly absorbed into the blood easily in the gastrointestinal tract. Instead, it is partially hydrolyzed in the gastrointestinal environment, and the hydrolyzed products are converted into beneficial metabolites such as short-chain fatty acids (SCFAs) by the intestinal flora to provide nutrients to

Address correspondence to Xiao Li, Xiaol_sunny@163.com; Wei Wang, 67445651@qq.com

intestinal mucosal cells and maintain the low pH enviroment in the gut. This further affects intestinal mucosal barrier function as well as the local and systemic immune systems[9]. It has been reported that *A. argyi* extract has remarkable suppressive effect on oxidative stress both *in vitro* and *in vivo*[10]. Polysaccharides from *A. argyi* could significantly improve the growth performance, regulate immune function and enhance the antioxidative capacity of broilers[11]. However, the effect of AAP on alleviating intestinal inflammation and regulating immune activity by acting on intestinal microorganisms has not been reported.

Currently, chemical inducers such as dextran sulfate sodium or trinitrobenzene sulfonic acid are commonly used to establish rodent models of intestinal inflammation; however, the degree of intestinal pathology is too high, rendering them unsuitable for the conduction of preventive studies to determine the role of dietary bioactive compounds[12]. Lipopolysaccharide (LPS) is the main component of the outer membrane of cell walls of gram-negative bacteria and can be recognized in animals by the Toll-like receptor (TLR) and nucleotide-binding oligomerization domain 2 (NOD2) receptor of intestinal wall antigen-presenting cells. LPS can activate the nuclear factor kappa light chain enhancer of activated B cells (NF-κB) inhibitory protein, initiate inflammatory pathways such as NF-κB, promote the expression of inflammatory factors, and elicit an intestinal inflammatory response. Moreover, LPS can selectively increase intestinal permeability by regulating tight-junction proteins, causing a pro-inflammatory state in the intestine and simulating mild intestinal inflammation[13,14]. Therefore, in this study, multiple intraperitoneal injections of LPS were used to establish a mouse model of intestinal inflammation. We used this model to study the protective effects of AAP in LPS-treated intestinal inflammation and barrier damage as well as to determine the relationship between AAP and intestinal flora, to provide a theoretical basis for the use of AAP as a potential active agent to treat intestinal inflammation.

2 Materials and methods

2.1 Chemicals and reagents

The leaves of *A. argyi* were collected in May 2022, from Nanyang County, Henan Province, China. LPS: Sigma Company in the United States; ELISA kits of tumor necrosis factor-α (TNF-α), interleukin-6 (IL-6), interleukin-17 (IL-17), and interleukin-1β (IL-1β): Shanghai Enzyme-Linked Biotechnology Co., Ltd.; superoxide dismutase (SOD), catalase (CAT), glutathione peroxidase (GSH-Px) and malondialdehyde (MDA) assay kits: Nanjing Jiancheng Bioengineering Institute; the TRIzol kit, RT Super Mix reverse transcription kit and SYBR® Premix Ex *Taq* kit: Takara Biomedical Technology (Beijing) Co., Ltd.; digestive enzyme assay kit: Beijing Solarbio Technology Co., Ltd. All other chemicals, reagents are pure analytical grade.

2.2 Preparation of AAP

The leaves of *A. argyi* were cut into 0.5 cm fragments. The fragments were degreased at 25 °C for 24 h with 95% ethanol (material-to-liquid ratio of 1:2) and filtered. Leaves of *A. argyi* were then separated by filtration. Next, ten times the volume of water was added and extracted twice at 100 °C for 1.5 h each time. Then filtered, combined, and concentrated the solution. 95% ethanol was added to the solution until the ethanol level was 85% (volume fraction). After allowing it to stand at 25 °C for 48 h, the precipitate was filtered. The free protein was removed using the Sevage method. AAP was obtained after dialysis, concentration, and freeze-drying.

2.3 Monosaccharide composition of AAP

The monosaccharides in AAP were determined using gas chromatography-mass spectrometry (GCMS-QP2010 Ultra, Shimadzu, Japan) and the external standard method[15]. The specific methods were as follows. Preparation of sample derivatives: 10 mg of AAP was weighed in an ampoule, 1 mL of 2 mol/L trifluoroacetic acid-methanol solution was added, and the ampoule was sealed with an alcohol blowtorch. The sample was hydrolyzed for 2 h in an oven at 120 °C, decompressed at 60 °C, spin steamed until dry, and dissolved in 200 μL water. Then, 1 mL of 0.5 mol/L sodium borohydride dimethylsulfoxide solution was added, mixed evenly, reacted at 40 °C for 90 min, and removed and cooled to room temperature. Next, 100 μL acetic acid, 200 μL 1-methylimidazole, and 1 mL acetic anhydride were added dropwise and acetylated at 40 °C for 10 min. Then, 2 mL distilled water was added and mixed well, followed by the addition of 2 mL chloroform to extract the acetylated products. The chloroform layer was washed again with 2 mL water, dried with 1 g anhydrous sodium sulfate, and filtered using a 0.22-μm organic filter membrane to obtain the sample derivative solution for GC-MS. It was performed on a Rtx-5MS capillary colomn (30 m × 0.25 mm, 0.25 μm).

2.4 Fourier-transform infrared (FT-IR) spectroscopy of AAP

Approximately 2 mg of AAP was weighed and an appropriate amount of potassium bromide powder was added. The sample was uniformly ground and pressed to form a pellet and analyzed using a Nicolet iN 10 FT-IR spectrophotometer (Madison, WI, USA). Scanning wavelength was set at 4,000–400 cm^{-1} (with 4 cm^{-1} resolution).

2.5 Animals and experimental design

Thirty Kunming mice were purchased from Henan Skbex Biotechnology Co., Ltd. All mice drink and eat freely for 1 week in a standard environment (temperature 20–25 °C, humidity 45%–50%). after 1 week of adaptive feeding, the mice were randomly and equally divided into the following 5 groups (6 mice per group): Normal control (NC), model control (MC), AAP low-dose (200 mg/kg, AL), AAP medium-dose (400 mg/kg, AM) and AAP high-dose (800 mg/kg, AH) groups. The experimental period lasted 21 days. On days 9, 13, 17, and 21, mice in the NC group were injected intraperitoneally with 0.2 mL normal saline; 0.2 mL of 1 mg/kg LPS was injected intraperitoneally into mice in other groups to induce intestinal inflammation and barrier injury[16,17]. From day 1 of the experiment, mice in the AL, AM, and AH groups were gavaged with 0.2 mL AAP solution once a day for the entire experimental period. Mice in the NC and MC groups received gavage of an equal volume of normal saline daily. The body weights of mice were measured on days 1, 7, 14, and 21, and the disease activity indices of mice were recorded daily and routinely. Experimental protocols were approved by the Animal Ethics of Henan Academy of Sciences (protocol code: HNP. No. 20230302001). The care and handling of animals were in compliance with the guidelines of the National Institutes of Health. All methods are reported in accordance with ARRIVE guidelines for the reporting of animal experiments.

2.6 Sample collection

On day 21 of the experiment, mice were euthanized by cervical dislocation and dissected 6 h after LPS treatment. The spleen and thymus tissues were isolated, collected and weighed. The immune organ index was calculated according to the following equation. Intestinal tissues and contents were collected for further analysis.

Immune organ index (‰) = weight of the organ (g)/body weight (g) × 1,000

2.7 Histopathology

The intestinal tissues were removed from the 4% paraformaldehyde solution. Approximately 1 cm of the middle segment was made and stained with hematoxylin-eosin (H&E), observed using a light microscopy (Olympus, DP-72, Tokyo, Japan). Images of the sections were obtained. The depths of the crypts for the ileum and colon, colonic fold height and jejunum villus length were recorded.

2.8 Reverse transcription-quantitative polymerase chain reaction (RT-qPCR)

The total RNA from ileum and colon mucosa was extracted using a TRIzol kit, and reverse transcription into cDNA was performed following the instructions in the reverse-transcription kit[18]. cDNA was used as a template for amplification and *β-actin* was used as reference. The expression of *Claudin-1*, *Occludin*, and Zonula occludens-1 (*ZO-1*) genes of the intestinal tissue was determined using an SYBR Premix Ex *Taq* kit. Reaction protocol: high-temperature denaturation at 95 °C for 5 min, renaturation at 95 °C for 15 s, annealing at 60 °C for 35 s, extension at 70 °C for 60 s; 40 cycles. The cycle threshold (Ct) value was used for relative quantification after RT-qPCR amplification. The Ct value method was used to determine the expression of target genes versus *β-actin* (Table 1).

2.9 ELISA

Intestinal tissues were prepared in a 1:10 ratio of weight (g) to volume (mL) in an ice-water bath, and the supernatant was centrifuged at 3,000 r/min for 15 min. The supernatant was collected, and the contents of TNF-α, IL-6, IL-17, IL-1β, SOD, CAT, GSH-Px, and MDA in intestinal tissues were measured per the instructions in the respective assay kits.

2.10 Western blotting

Colon tissues were lysed with RIPA lysate buffer and the supernatant was collected after centrifugation. Protein concentrations were measured using a bicinchoninic acid assay kit, followed by sodium dodecyl sulfate-polyacrylamide gel electrophoresis. The protein blots were transferred to a microporous polyvinylidene difluoride membrane (Millipore, MA, USA). The membranes were blocked with 5% skimmed milk at room temperature for 2–3 h, washed in Tris-buffered saline and Tween 20 buffer, incubated with the primary antibodies for p65 NF-κB and IκBα at 1:500 dilution with 5% skimmed milk, and shaken overnight at 4 °C. The membranes were then incubated with the corresponding secondary antibodies for 2 h. Enhanced chemiluminescence solution was added in the dark and the membranes were photographed using a gel imaging system. The gray value of each protein band was analyzed using ImageJ software and the relative expression of target proteins was calculated (using *β*-actin as the internal reference).

2.11 SCFA content in feces

The colon contents of mice were accurately weighed and five volumes of methanol were added. The mixture was stirred into suspension. Adjust the pH to 2–3, the samples were centrifuged at 12,000 r/min for 10 min, the supernatant was used to determine SCFA content. The instrument used to determine the content of SCFA was gas chromatograph (Shimadzu, Japan) equipped with a DB-FFAP capillary column (30 m × 0.25 mm, 0.25 μm).

2.12 16S rRNA high-throughput sequencing to determine the abundance of intestinal flora

The colonic contents were analyzed using 16S rRNA high-throughput sequencing, commissioned by Shanghai Parsono Biotechnology Co., Ltd. (China).

2.13 Statistical analysis

Microsoft Excel was used for preliminary statistical analyses. GraphPad Prism 8 was used for image processing. All experiments were conducted in triplicate and the average values were used for analysis. Comparisons to determine significant differences were performed using one-way analysis of variance and Duncan's multiple comparisons using SPSS 22.0 software.

3 Results

3.1 Isolation and purification of AAP

AAP was obtained after degreasing with 95% ethanol, hot water extraction, ethanol sedimentation, deproteinization, dialysis, concentration, and lyophilization. The yield of AAP was 1.02%, based on the dry weight of the crude polysaccharides. The polysaccharide content in AAP was determined to be 86.0% using the sulfuric acid-phenol method. The protein content was determined to be 2.15% using the Coomassie brilliant blue method.

3.2 Determination of the monosaccharide composition of AAP

The levels of the seven monosaccharide derivatives were determined using GC-MS. The monosaccharides of AAP were rhamnose, xylose, arabinose, mannose, glucose, and galactose (Table 2), and they were in a molar ratio of 0.49 : 0.21 : 0.43 : 0.29 : 1.00 : 0.18.

Table 1 Primer sequence

Gene Name	Forward primer	Reverse primer
Claudin-1	5'-AGATACAGTGCAAAGTCTTCGA-3'	5'-CAGGATGCCAATTACCATCAAG-3'
Occludin	5'-TGCTTCATCGCTTCCTTAGTAA-3'	5'-GGGTTCACTCCCATTATGTACA-3'
ZO-1	5'-CTGGTGAAGTCTCGGAAAAATG-3'	5'-CATCTCTTGCTGCCAAACTATC-3'
β-actin	5'-CTACCTCATGAAGATCCTGACC-3'	5'-CACAGCTTCTCTTTGATGTCAC-3'

Table 2 Monosaccharide composition of AAP ($n = 3$)

Rhamnose	Xylose	Arabinose	Mannose	Glucose	Galactose
18.85 ± 0.24	8.08 ± 0.07	16.54 ± 0.15	11.15 ± 0.10	38.46 ± 0.52	6.92 ± 0.24

3.3 FT-IR of AAP

FT-IR is a commonly used method to determine the structure of polysaccharides. It is used to identify the functional groups and their amounts in polysaccharides based on the peak shape and peak intensity of the generated spectrum[19]. The characteristic absorption peak of the polysaccharide appears at 2,000–800 cm^{-1}, and a strong and wide characteristic absorption peak at 3,420 cm^{-1} indicates the presence of –OH tensile vibration. The peak at 2,926 cm^{-1} is attributed to the –CH tensile vibration, whereas the absorption peak at 1,630 cm^{-1} indicates the presence of COO–R in AAP[20]. The strong and wide absorption peak near 1,074–1,042 cm^{-1} corresponds to the stretching vibration between the C–O and C–C bonds and the bending vibration of C–OH in the pyranose ring[21]. The absorption peak in the 950–800 cm^{-1} region is due to C–H bending, and the absorption peak at 896 cm^{-1} indicates the presence of the β-configuration glycosidic bond[22]. The infrared spectrum of AAP is shown in Fig. 1.

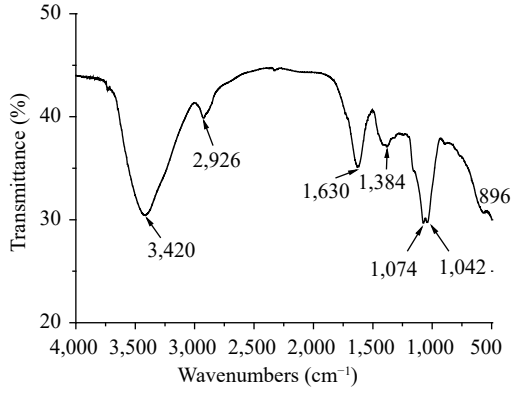

Figure 1 Infrared spectrum of AAP.

3.4 Effects of AAP on the body weight and the spleen and thymus indices

There were no significant differences in the body weights of mice before the intraperitoneal injection of LPS. After LPS injection, the increase in body weights of mice in the MC group decreased significantly ($P < 0.01$) compared with that in the NC group (Fig. 2). Mice in the MC group exhibited a reduction in diet intake, lethargy, unformed stool, eye secretions, and messy fur. The spleen and thymus indices, body weight gain in the MC group decreased significantly ($P < 0.01$) compared with those in the NC group, indicating the successful establishment of the model. The body weight gain in AL, AM, and AH groups increased significantly ($P < 0.01$) compared with that in the MC group (Fig. 2A), indicating that AAP could inhibit the decrease in body weight after LPS injection. The body weight gain was proportional to the AAP dose. The spleen and thymus indices of AAP group increased, and the increase in the AM and AH groups was significant ($P < 0.01$) (Fig. 2B). The results indicated that AAP could improve atrophy in LPS-treated immunosuppressed mice, promote spleen and thymus growth, and protect the immune organs.

3.5 Changes of intestinal inflammatory factors and oxidative indices

ELISA was used to examine four kinds of inflammatory factors (TNF-α, IL-6, IL-17, and IL-1β) and oxidative indices (SOD, CAT, GSH-Px, and MDA) in intestinal tissues respectively, to evaluate the action of AAP. The results were represented in Fig. 3. The levels of TNF-α, IL-17, and IL-1β in the ileum and colon tissues increased extremely significantly ($P < 0.01$) (Fig. 3A), and IL-6 levels in ileum tissues increased significantly ($P < 0.05$) compared with those in the NC group. After AAP intervention, the levels of TNF-α, IL-6, IL-17, and IL-1β decreased to different extents compared with those in the MC group.

Compared with those in the NC group, SOD and GSH-Px activities in the ileum and colon tissues decreased significantly ($P < 0.01$) in the MC group (Fig. 3B); MDA activity increased significantly ($P < 0.01$); and CAT activity in the colon decreased significantly ($P < 0.01$). SOD and CAT activities in the AH group increased significantly ($P < 0.01$); MDA activity in the AM and AH groups decreased significantly ($P < 0.01$); SOD, CAT, and GSH-Px activities in the AL and AM groups increased to different extents; and MDA activity in the AL group decreased compared with those in the MC group. These results indicated that AAP could restore the oxidative stress system in intestinal tissues by increasing the activities of SOD, CAT, and GSH-Px, and reducing MDA levels.

3.6 Changes of intestinal mucosal barrier

HE staining was used to detect the pathological changes of

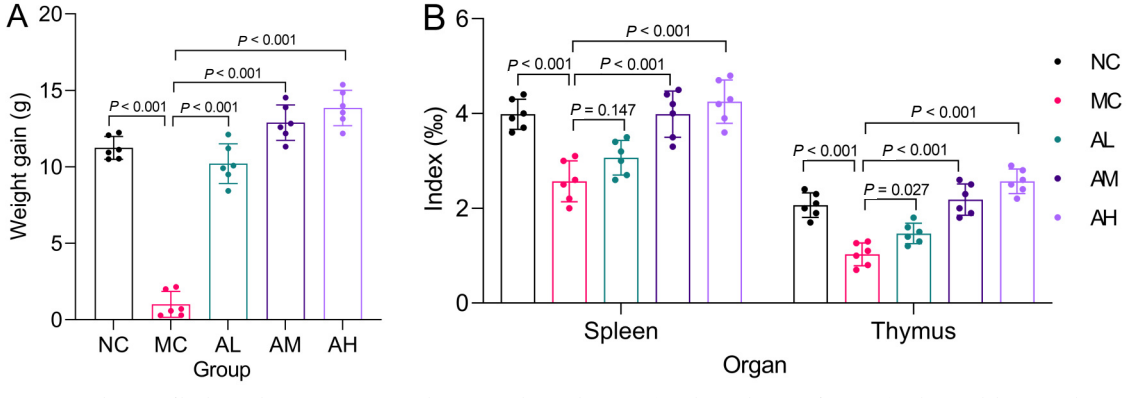

Figure 2 Changes of body weight, immune organ index in mice during the test. (A) Body weight gain of mice, (B) Spleen and thymus index.

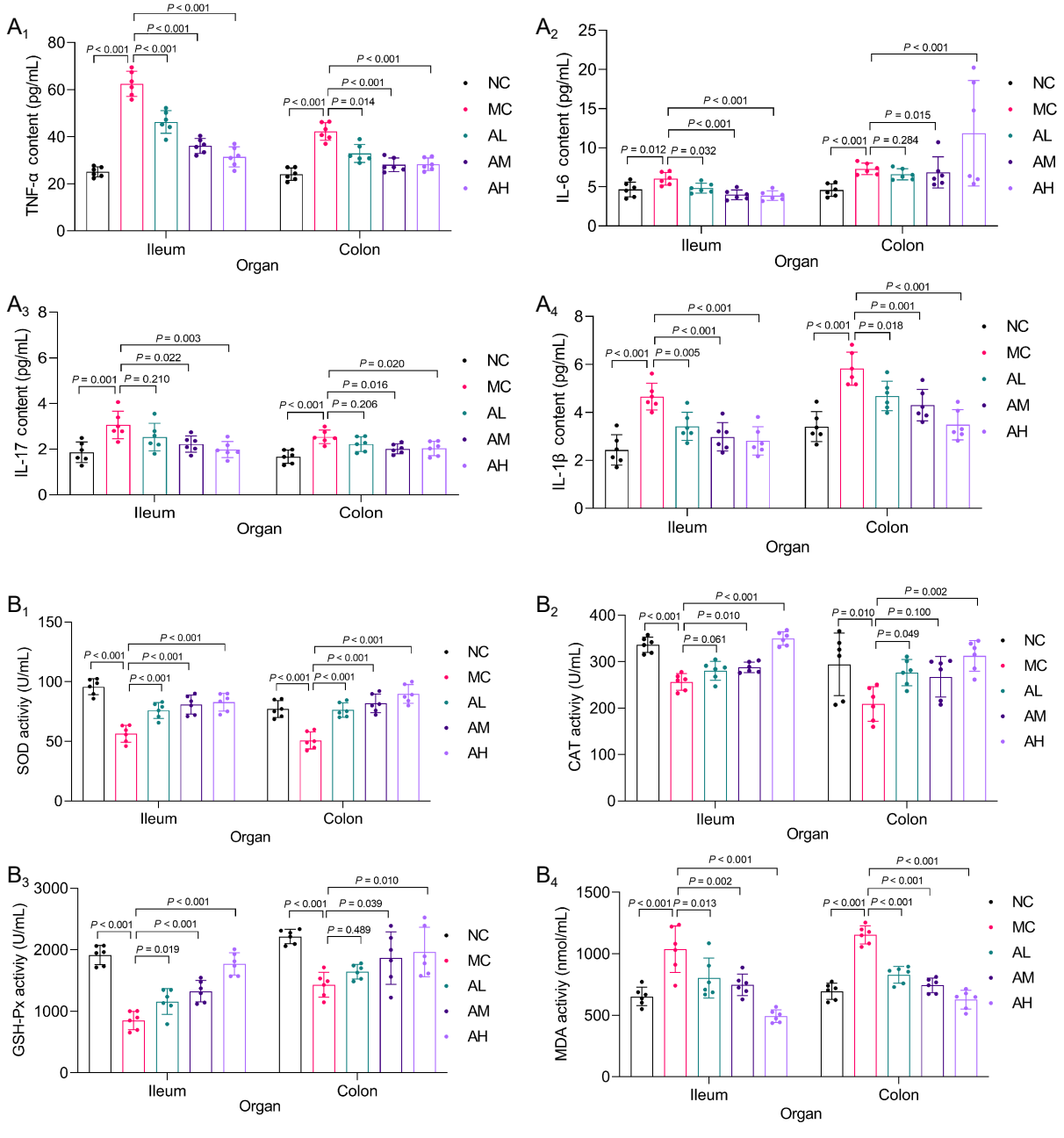

Figure 3 Changes of intestinal inflammatory factors and oxidative indices. (A_1-A_4) TNF-α, IL-6, IL-17 and IL-1β levels in the ileum and colon, (B_1-B_4) SOD, CAT, GSH-Px and MDA activities in the ileum and colon.

ileum and colon tissues (Fig. 4). Figures 4A, 4B show that the intestinal mucosa in the NC group is intact with clearly visible crypts and normal epithelial cell morphology. Ileum villi atrophy is shorter with wide spacing in the MC group; moreover, muscular layer atrophy is observed. A part of the intestinal glands of the colon appears necrotic and detached from the basement membrane. In the AAP-treated groups, the intestinal morphology improved, crypt morphology and goblet cells appeared intact, villi length increased, and mucosal damage was reduced. The ileum villi length, crypt depth, colonic fold height, and crypt depth were measured (Fig. 4C). The ileum villi length, fold height, colonic recess depth, and fold height in the MC group decreased significantly ($P < 0.01$) compared with those in the NC group, indicating that LPS caused intestinal villi injury, shallow recesses, and damage to the intestinal mucosal barrier. The AAP-treated groups showed different extents of improvement compared with the MC group. In the AH group, the ileum villi length and colonic crypt depth increased significantly ($P < 0.01$), and colonic crypt depth a significant level ($P < 0.05$). The ileum villi length, crypt depth, and colonic fold height increased significantly ($P < 0.05$) in tissues in the AM group. The ileum recess depth increased significantly ($P < 0.05$) in tissues in the AL group. These results indicated that AAP could repair LPS-treated intestinal damage, by improving the intestinal morphology of LPS-treated mice, and increase the ileum villi length, crypt depth, colonic fold height, and crypt depth.

3.7 Changes of intestinal tight-junction proteins

Intestinal inflammation is often accompanied by changes in intestinal tight-junction protein levels[23]. In this study, RT-qPCR

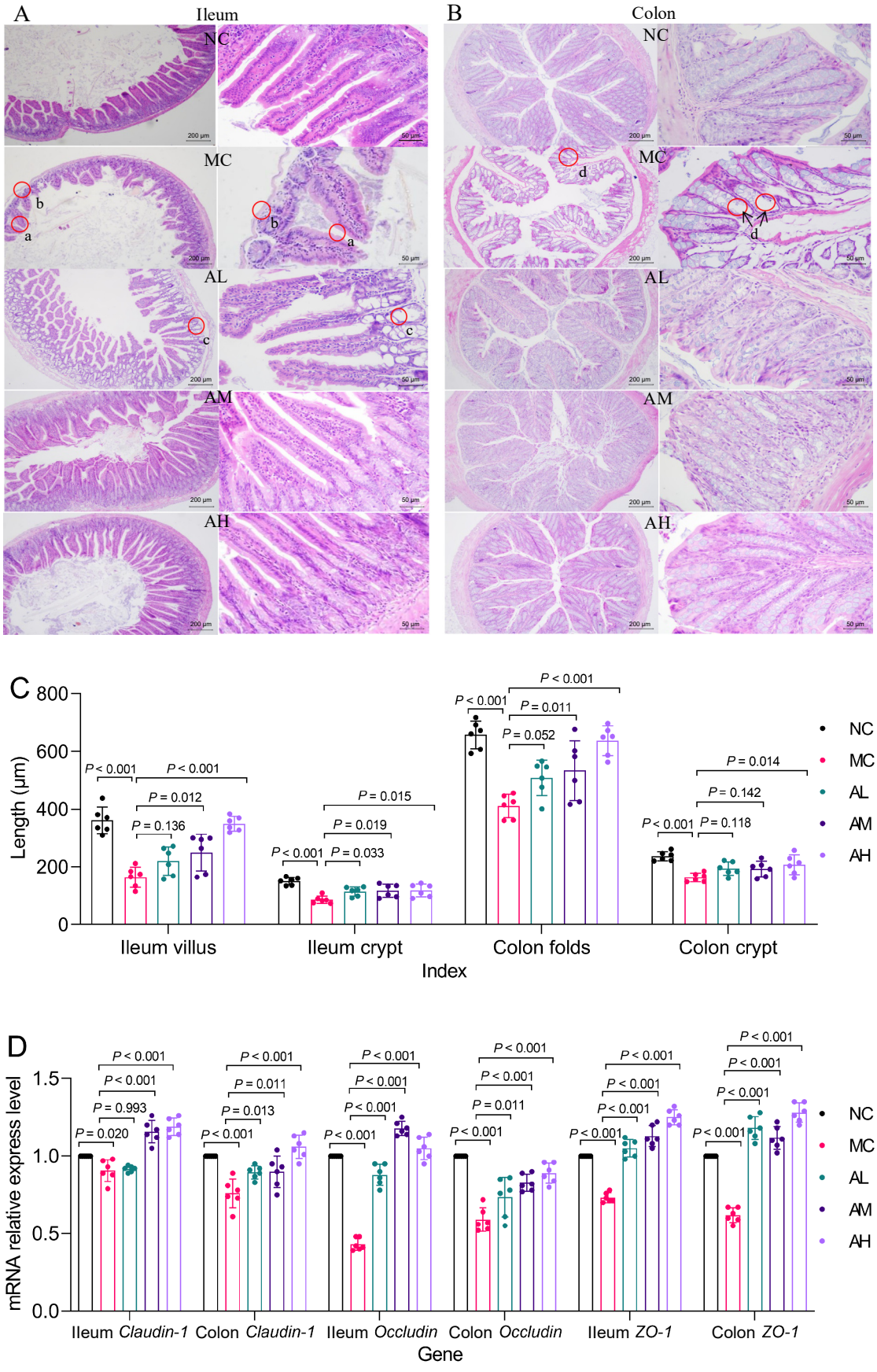

Figure 4 Changes of intestinal mucosal barrier. (A) Histopathological changes of mice ileum sections; magnification 10× (A_1) and 40× (A_2), (B) Histopathological changes of mice colon sections; magnification 10× (B_1) and 40× (B_2), a. The ileum villi atrophy became shorter; spacing widening; b. The muscular layer atrophy; c. Part of the intestinal glands of the ileum are necrotic and cryptic fusion; d. The base of the colon intestinal glands are necrotic, (C) Villus length and crypt depth of ileum, folds height and crypt depth of colon, (D) Changes of intestinal tight-junction proteins (mRNA relative expression level of *Claudin-1*, *Occludin*, and *ZO-1*).

was used to determine the relative mRNA expression of the intestinal barrier-related junction proteins *Claudin-1*, *Occludin*, and *ZO-1* (Fig. 4D). The relative mRNA expression of *Claudin-1*, *Occludin*, and *ZO-1* in the ileum and colon mucosa decreased in the MC group compared with that in the NC group. The relative mRNA expression of *Claudin-1*, *Occludin*, and *ZO-1* of AAP group increased to different extents compared with that of mice in the MC group. The relative *Occludin* and *ZO-1* in the AM and AH groups increased significantly ($P < 0.01$). Also, the relative *Claudin-1* in the ileum and colon of AH group increased significantly ($P < 0.01$). These results indicated that LPS significantly decreased the expression of *Claudin-1*, *Occludin*, and *ZO-1*, increased the permeability of the intestinal epithelium; which was consistent with the pathological findings in the intestinal sections as well as with the symptoms of diarrhea in mice. AAP could decrease intestinal permeability and relieve the symptoms of LPS-treated diarrhea by upregulating the above proteins, and maintaining the integrity of the intestinal barrier.

3.8 Regulation of signal pathway expression by AAP

NF-κB plays an important role in inflammatory and immune responses[24]. To elucidate the mechanism of LPS-treated intestinal injury in mice, we studied the activation of the NF-κB signaling pathway. Western blotting revealed that compared with that in the NC group, the expression of p65 NF-κB in the MC group was significantly upregulated ($P < 0.01$) and the expression of IκBα was downregulated ($P < 0.01$). The analysis revealed that LPS activated the NF-κB signaling pathway. p65 NF-κB expression was significantly downregulated ($P < 0.01$) and IκBα expression was significantly upregulated ($P < 0.01$) in a dose-dependent manner (Fig. 5) in the AAP groups. It revealed that AAP may inhibit the production of inflammatory factors TNF-α, IL-6, IL-17, and IL-1β in intestinal tissues by blocking the degradation of IκBα and phosphorylation of p65.

3.9 Changes of intestinal SCFA levels

SCFAs are main metabolites of the intestinal flora, among the various microbial metabolites, acetic acid, butyric acid, and propionic acid are the key bacterial metabolites that promote the development and maintenance of the immune system[25]. In the study, SCFA levels in mice colons were determined. The rusults showed their levels were lower (acetic acid, propionic acid, and butyric acid) in the MC group. The levels of acetic acid and propionic acid in the AL group increased significantly ($P < 0.05$) and the content of butyric acid increased extremely significantly ($P < 0.01$) compared with those in the MC group. The levels of acetic acid, propionic acid, and butyric acid in the AM and AH groups increased significantly ($P < 0.01$) versus those in the MC group (Fig. 6). These results indicated that AAP intervention could increase SCFA levels in the intestinal tract of LPS-treated mice.

3.10 Changes of intestinal flora

16S rRNA sequencing was used to determine the species and abundances of intestinal microorganisms. Alpha diversity was determined to assess species abundance and diversity. We found that Chao1 in the AL, AM, and AH groups was higher than that in the MC group, indicating that AAP could increase the abundance of intestinal flora in LPS-treated mice. The Shannon and Simpson diversity indices of the treated groups were higher than those of the NC and MC groups, indicating that the AAP intervention could improve the diversity of intestinal flora in LPS-treated mice (Fig. 7A). Exclusivity analysis of operational taxonomic units (OTUs) revealed 10,652 OTUs obtained by comparison, with 90%, 33%, and 15% annotated to the phylum, genus, and species levels, respectively. The number of species in the AAP and NC groups were both higher than that in the MC group (Fig. 7B).

The composition of the intestinal flora at the phylum level, genus level and species level were explored. At the phylum level, the main components of the five groups included thick-walled phyla Firmicutes, Bacteroidetes, Proteobacteria, and Actinobacteria. Firmicutes and Bacteroidetes accounted for more than 90% of the total microorganisms (Fig. 8A). Compared with that in the NC group, the relative abundance of Firmicutes in the MC group was significantly decreased ($P < 0.05$), whereas the relative abundance of Proteobacteria was significantly increased ($P < 0.05$). The abnormal increase in Proteobacteria abundance led the intestinal microbiota to an imbalanced state. Moreover, this increase in Proteobacteria was considered a potential characteristic of disease risk[26]. After AAP intervention, the relative abundance of Proteobacteria in the AM and AH groups was significantly decreased ($P < 0.05$) and the relative abundance of Firmicutes was extremely significantly increased ($P < 0.01$) compared with that in the MC group.

Most bacteria belonging to the Firmicutes phylum, such as *Lactobacillus*, fecal *Bacillus*, and Roche *Bacillus*, are beneficial as they produce butyric acid in the intestinal tract and maintain intestinal health[27]. The study indicated that AAP could reduce the relative expression of 16S rRNA gene in Proteobacteria, increase the relative abundance of Firmicutes, regulate the composition of the intestinal flora.

Lactobacillus is the primary genus of intestinal flora in mice,

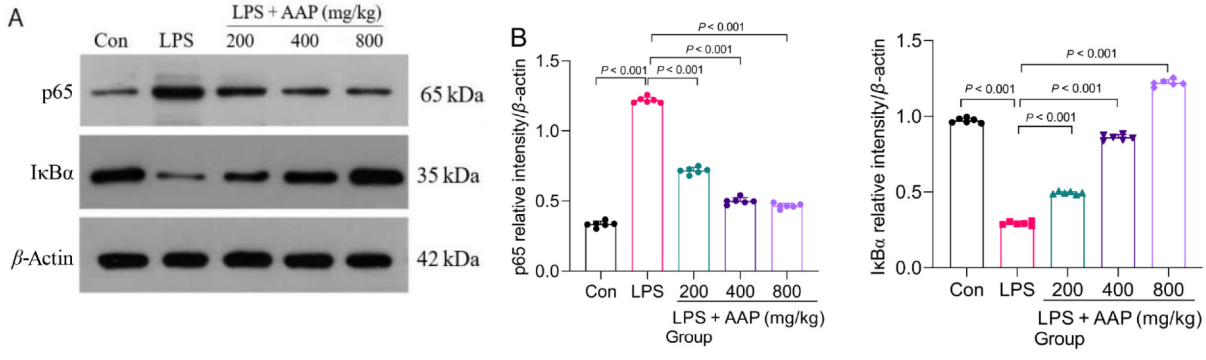

Figure 5 Effect of AAP on the expression levels of p65 NF-κB and IκBα proteins in mice colon. (A) Western blot analysis of p65 NF-κB, IκBα expression, (B) Densitometry was performed to quantify the levels of the proteins. Compared with group NC (Con).

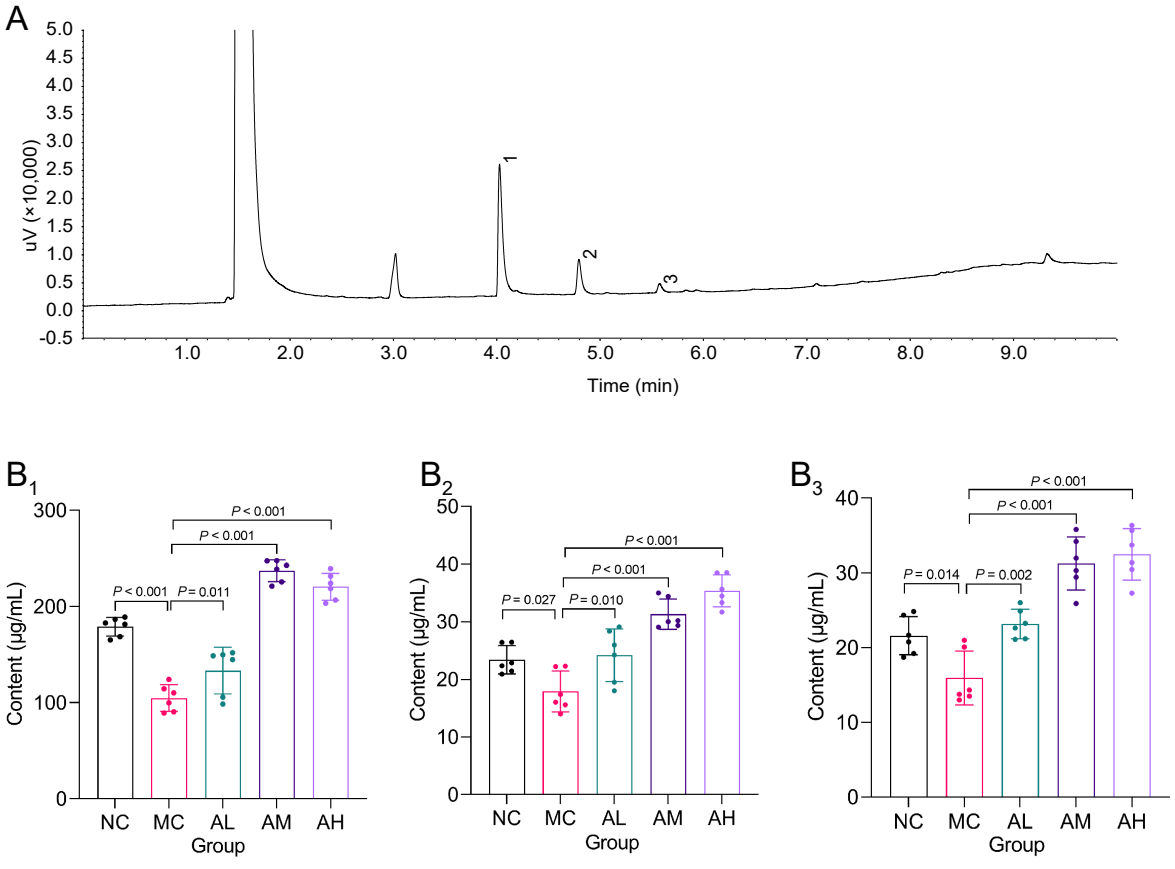

Figure 6 Changes of SCFAs. (A) GC chromatogram of sample. 1. Acetic acid, 2. propionic acid, 3. butyric acid, (B) Contents of SCFAs in mice. (B_1-B_3) Acetic acid, propionic acid, butyric acid.

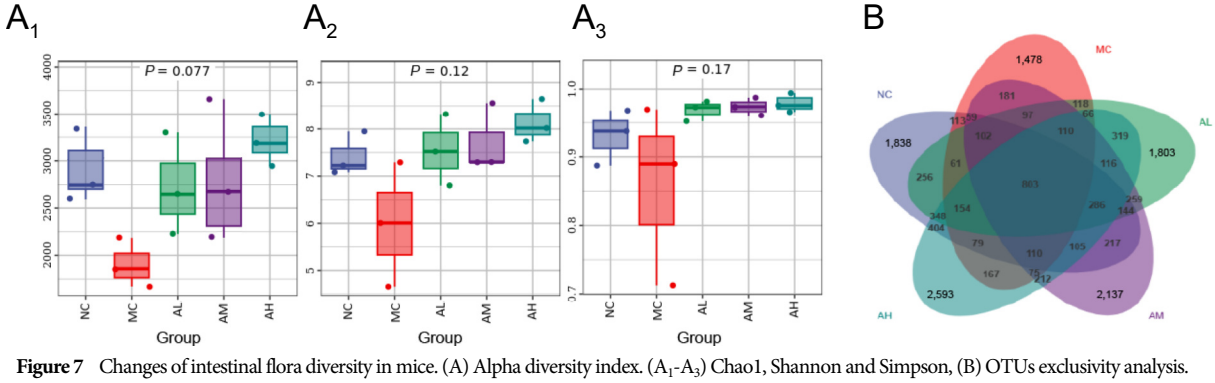

Figure 7 Changes of intestinal flora diversity in mice. (A) Alpha diversity index. (A_1-A_3) Chao1, Shannon and Simpson, (B) OTUs exclusivity analysis.

followed by *Bacteroides* and *Prevotella* (Fig. 8B). The abundance of *Lactobacillus* was significantly decreased ($P < 0.05$) and the abundance of *Prevotella* was significantly increased ($P < 0.05$) in the MC group compared with that in the NC group. After AAP intervention, *Lactobacillus* abundance in the AH group was significantly increased ($P < 0.05$) and *Prevotella* abundance was significantly decreased in the AH group ($P < 0.05$) compared with that in the MC group.

The intestinal microorganisms present at high abundance included *Lactobacillus_hamsteri*, *Lactobacillus_vaginalis*, *Bacteroides_acidifaciens*, *Desulfovibrio*, *Mucispirillum schaedleri*, *Akkermansia_muciniphila*, and *Lactobacillus_salivarius*. *Lactobacillus* and *Akkermansia* were decreased in the MC group, whereas *Desulfovibrio* was significantly increased ($P < 0.05$) versus that in the NC group. After AAP intervention, the abundances of both *Lactobacillus* and *Akkermansia* were improved and that of *Desulfovibrio* was significantly decreased ($P < 0.05$) compared with MC group. Cluster analysis revealed that the diversity and abundance of intestinal flora in AAP and NC groups were different from those in MC group, the structural composition of the intestinal flora in the AAP group to be better (Fig. 8C). The study revealed that AAP could make great effects in regulating the intestinal flora balance in LPS-treated mice, with especially obvious in the AH group.

3.11 Correlation between intestinal microorganisms and tight-junction proteins, SCFAs, antioxidant indices, and inflammatory factors

Correlation results are shown in Fig. 9. The relative abundance

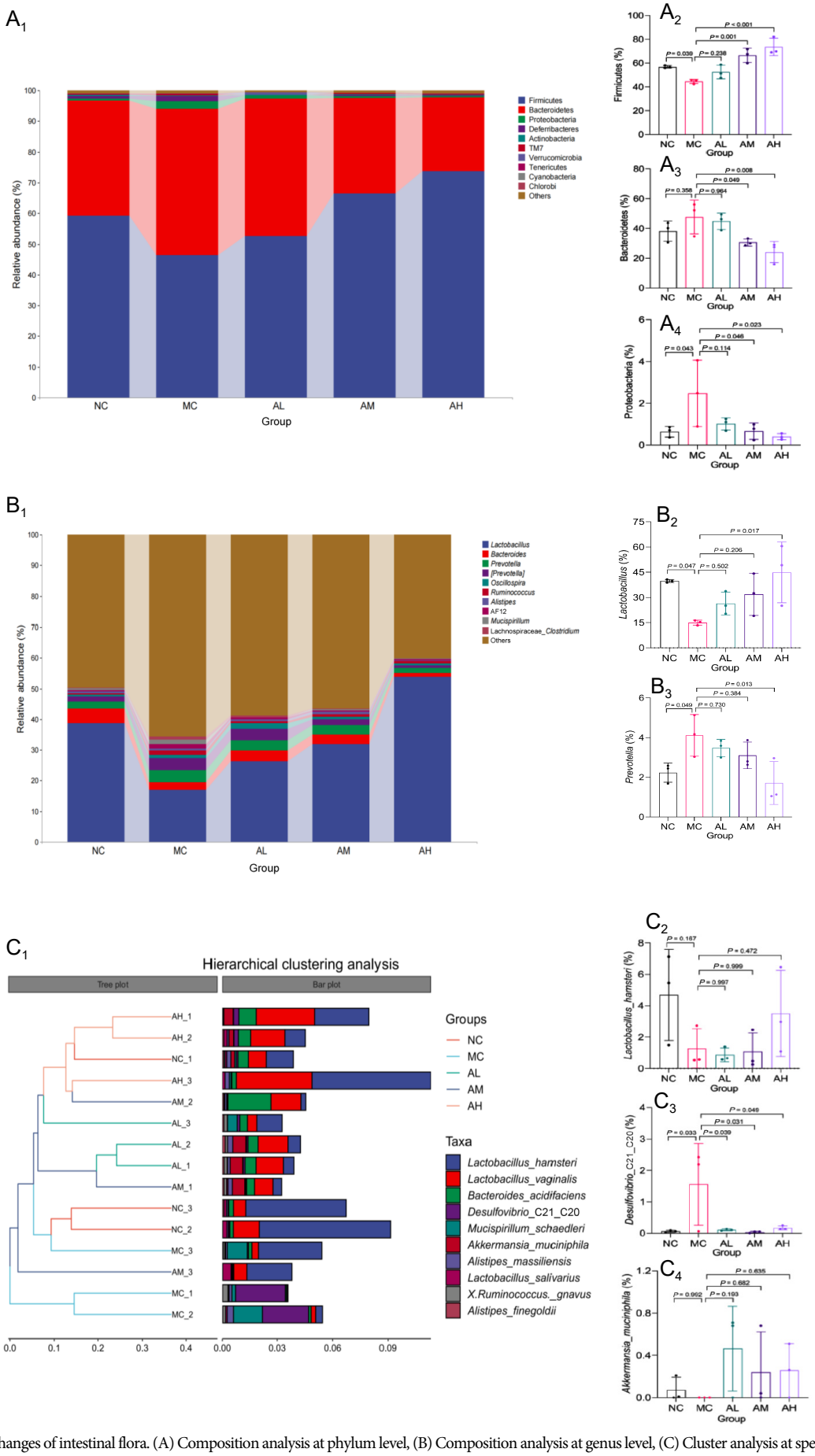

Figure 8 Changes of intestinal flora. (A) Composition analysis at phylum level, (B) Composition analysis at genus level, (C) Cluster analysis at species level.

of Firmicutes, *Lactobacillus*, and *Lactobacillus_hamsteri* was positively correlated with the intestinal barrier-related proteins *Claudin-1*, *Occludin*, and *ZO-1*, and with SCFA, SOD, CAT, and GSH-Px activities; and negatively correlated with MDA, TNF-α, IL-6, IL-17, and IL-1β. However, the relative abundance of Proteobacteria, *Prevotella*, *Desulfovibrio*, and *M. schaedleri* was negatively correlated with the intestinal barrier-related proteins *Claudin-1*, *Occludin*, and *ZO-1*, as well as with SCFA, SOD, CAT, and GSH-Px activities, but positively correlated with MDA and the inflammatory factors TNF-α, IL-6, IL-17, and IL-1β (Fig. 9A). In the MC group, the relative abundance of Proteobacteria, *Prevotella*, *Desulfovibrio*, and *M. schaedleri*, and the levels of MDA, TNF-α, IL-6, IL-17, and IL-1β were higher. The abundance of Firmicutes, *Lactobacillus*, and *Lactobacillus_hamsteri*, and the levels of *Claudin-1*, *Occludin*, *ZO-1*, SCFAs, SOD, CAT, and GSH-Px were lower. After AAP intervention, all indices changed

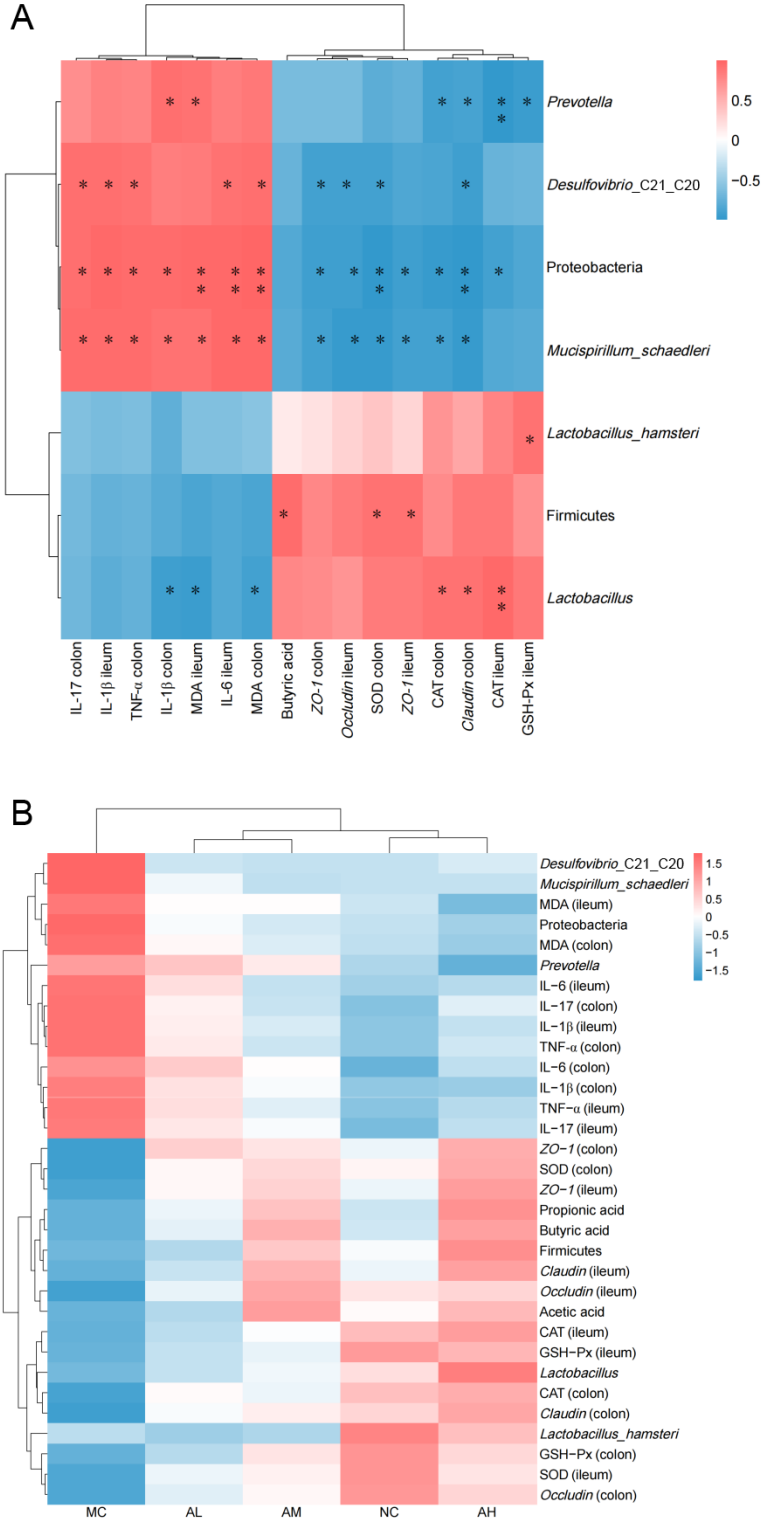

Figure 9 Correlation analysis. (A) Correlation analysis of intestinal flora, (B) Correlation analysis of group. Red indicates positive correlation and blue indicates negative correlation. * $P < 0.05$, ** $P < 0.01$.

to different extents compared with those in the MC group, and the most obvious improvement was noted in the AH group: the abundance of Proteobacteria, *Prevotella*, *Desulfovibrio*, and *M. schaedleri*, and the levels of MDA, TNF-α, IL-6, IL-17, and IL-1β decreased. The abundance of Firmicutes, *Lactobacillus*, and *Lactobacillus_hamsteri*; and levels of *Claudin-1*, *Occludin*, *ZO-1*, and SCFAs; and SOD, CAT, and GSH-Px activities increased (Fig. 9B). Combined with the previous compositional changes in the intestinal flora, AAP intervention significantly increased the relative abundance and proportion of beneficial bacteria to different extents, improved SCFA levels, increased the expression of intestinal tight-junction proteins, enhanced antioxidant activity, inhibited the release of inflammatory factors, and alleviated LPS-treated intestinal inflammation and barrier damage.

4 Discussion

The present study preliminarily explored the potential mechanisms of AAP in alleviating intestinal inflammation in mice, AAP against intestinal inflammation was investigated including its effects on protecting immune organs, inhibiting oxidative stress response, regulation of inflammatory signaling pathway, and abundance of intestinal probiotics in mice, etc.

The overexpression of inflammatory factors is one of the main signs of intestinal diseases. TNF-α can increase intestinal permeability by affecting the integrity of intestinal epithelial cells[28, 29]. IL-6 is a multifunctional pro-inflammatory factor, with multiple inflammatory factors playing a synergistic role; it is often used as an indicator to assess disease severity[30]. IL-17, IL-1β are main pathogenic factors of intestinal inflammation and plays an important role in intestinal homeostasis regulation[31, 32]. Reducing the release of inflammatory factors and regulating the level is one of the effective ways to treat intestinal inflammation. In this study, AAP was found could reduce the hypersecretion of the inflammatory factors TNF-α, IL-6, IL-17, and IL-1β in LPS-treated intestinal tissues, thus inhibiting the occurrence and development of the inflammatory response.

The formation of oxidative stress in the gut and the destruction of the antioxidant enzyme system are also considered to be one of the pathogenesis of intestinal inflammation. During oxidative stress, the adhesion of intestinal epithelial cells to probiotics decreases, the intestinal barrier is destroyed, and infection by pathogenic bacteria increases[33]. Many researches have shown that natural polysaccharides have enhanced antioxidant activity in immunosuppressed mice[34, 35]. It has been found the addition of AAP in diets increased the activity of intestinal mucosal antioxidant enzymes (GSH-Px, SOD, CAT) and successfully inhibited lipid peroxidation and reduced MDA content in broilers[11]. In this study, SOD, CAT, GSH-Px, and MDA are used as the evaluation index of oxidative stress in the body. The indexes in the high dose group were significantly different ($P < 0.01$) compared with those in the model group. The results are in agreement with the existing literature on AAP.

Substantial evidence suggests that intestinal epithelial permeability plays a critical role in the onset and progression of intestinal diseases[36]. Tight-junction proteins are located at the apex of intestinal epithelial cells and are major determinants of barrier permeability in this cell type. Tight junctions are composed of transmembrane proteins such as *Claudin-1* and *Occludin*, peripheral membrane proteins such as *ZO-1*, and regulatory proteins[37]. We found that LPS significantly decreased the expression of *Claudin-1*, *Occludin*, and *ZO-1*, increasing the permeability of the intestinal epithelium. AAP could significantly increase the expression of these proteins, which was consistent with the pathological findings in the intestinal sections as well as with the symptoms of diarrhea in mice. These results suggested that AAP could decrease intestinal permeability and relieve the symptoms of LPS-treated diarrhea by upregulating the expression of intestinal tight-junction proteins and maintaining the integrity of the intestinal barrier.

NF-κB is the central regulator of immune and inflammatory response factors, whereas p65 is the important protein controlling NF-κB transcription. p65 NF-κB is inactive during normal physiological conditions; it combines with IκBα to prevent the expression of inflammatory cytokines[38]. Stimulation by external factors such as LPS leads to a cascade reaction wherein the NF-κB signaling pathway is activated and IκBα is degraded by protease, thus enabling the entry of p65 NF-κB into the nucleus to regulate the expression of related inflammatory cytokines and genes[39]. Western blotting showed that LPS could activate the NF-κB signaling pathway, whereas AAP intervention blocked IκBα degradation and p65 phosphorylation, thereby inhibiting the production of inflammatory cytokines in intestinal tissues, improving the immunomodulatory function of mice.

SCFAs are the main metabolites resulting from the anaerobic fermentation of intestinal prebiotics. Acetic acid, butyric acid, and propionic acid are the key bacterial metabolites among various microbial metabolites. They lower the pH in the colon, which is beneficial for the growth of probiotic bacteria and in promoting intestinal health. Butyric acid, in particular, is a major energy source for intestinal mucosal cells, which not only increases the abundance of lactobacilli but also reduces the number of colon bacilli, thereby alleviating intestinal diseases[9]. We found that AAP could significantly increase and upregulate the levels of acetic acid, propionic acid, and butyric acid in the intestine, which was helpful in improving the composition of the intestinal microbiota, promoting the repair of the intestinal mucosa, and restoring intestinal function.

The intestinal flora plays an important role in regulating immune function. Intestinal inflammatory diseases are accompanied by disturbances in the intestinal flora composition, which affects physiological processes such as energy metabolism, immune regulation in humans[40]. Therefore, to eliminate inflammatory symptoms and treat intestinal inflammatory diseases, it is particularly important to restore the composition of the intestinal flora. Most bacteria belonging to the Firmicutes phylum, such as *Lactobacillus*, fecal *Bacillus*, and Roche *Bacillus*, are beneficial as they produce butyric acid in the intestinal tract and maintain intestinal health[41]. The results of our study indicate that AAP could increase the relative abundance of Firmicutes, reduce the relative expression of 16S rRNA gene in Proteobacteria, regulate the composition of the intestinal flora, and restore the balance of the intestinal flora in LPS-treated mice. Meanwhile, AAP can improve metabolism and promote the proliferation of intestinal probiotics, inhibit the growth of harmful bacteria such as Proteobacteria, regulate the intestinal microecological balance, maintain the abundance and diversity of the intestinal flora.

Results from correlation analysis showed that beneficial intestinal bacteria such as Firmicutes, *Lactobacillus*, and *Lactobacillus_hamsteri* were positively correlated with the activities of the intestinal mucosal barrier related proteins, SCFAs, SOD, CAT, and GSH-Px, and negatively correlated with the levels of MDA and inflammatory factors; all indices were changed obviously in the high group.

5 Conclusions

AAP could regulate the composition of the intestinal flora in LPS-treated mice, increase bacterial abundance, improve the intestinal environment, reduce intestinal inflammation, repair the intestinal mucosal barrier, and restore intestinal function. These aspects highlight the potential of AAP and warrant its development and use in the prevention and treatment of intestinal inflammatory diseases.

Conflicts of interest

The authors declare that there are no conflicts of interest.

Acknowledgements

The authors gratefully acknowledge the financial support provided by Major Research Project of Henan Academy of Sciences (No. 210113003).

References

[1] Ng, S. C., Shi, H. Y., Hamidi, N., et al. Worldwide incidence and prevalence of inflammatory bowel disease in the 21st century: a systematic review of population-based studies. *The Lancet*, **2017**, 390: 2769–2778. https://doi.org/10.1016/S0140-6736(17)32448-0

[2] Okumura, R., Takeda, K. Roles of intestinal epithelial cells in the maintenance of gut homeostasis. *Experimental & Molecular Medicine*, **2017**, 49: e338. https://doi.org/10.1038/emm.2017.20

[3] Lan, T., Tang, T., Li, Y., et al. FTZ polysaccharides ameliorate kidney injury in diabetic mice by regulating gut-kidney axis. *Phytomedicine*, **2023**, 118: 154935. https://doi.org/10.1016/j.phymed.2023.154935

[4] Liang, Q., Zhao, Q., Hao, X., et al. The Effect of *Flammulina velutipes* polysaccharide on immunization analyzed by intestinal flora and proteomics. *Frontiers in Nutrition*, **2022**, 9: 841230. https://doi.org/10.3389/fnut.2022.841230

[5] Yu, Y., Mendoza, T. M., Ribnicky, D. M., et al. An extract of Russian tarragon prevents obesity-related ectopic lipid accumulation. *Molecular Nutrition & Food Research*, **2018**, 62: e1700856. https://doi.org/10.1002/mnfr.201700856

[6] Li, S., Zhou, S., Yang, W., et al. Gastro-protective effect of edible plant *Artemisia argyi* in ethanol-induced rats via normalizing inflammatory responses and oxidative stress. *Journal of Ethnopharmacology*, **2018**, 214: 207–217. https://doi.org/10.1016/j.jep.2017.12.023

[7] Cui, D., Ma, J., Liang, T., et al. Selenium nanoparticles fabricated in laminarin polysaccharides solutions exert their cytotoxicities in HepG2 cells by inhibiting autophagy and promoting apoptosis. *International Journal of Biological Macromolecules*, **2019**, 137: 829–835. https://doi.org/10.1016/j.ijbiomac.2019.07.031

[8] Zhang, P., Shi, B., Li, T., et al. Immunomodulatory effect of *Artemisia argyi* polysaccharide on peripheral blood leucocyte of broiler chickens. *Journal of Animal Physiology and Animal Nutrition*, **2018**, 102: 939–946. https://doi.org/10.1111/jpn.12895

[9] Chen, S., Wang, J., Fang, Q., et al. A polysaccharide from natural *Cordyceps sinensis* regulates the intestinal immunity and gut microbiota in mice with cyclophosphamide-induced intestinal injury. *Food & Function*, **2021**, 12: 6271–6282. https://doi.org/10.1039/d1fo00596k

[10] Zhang, P., Sun, D., Shi, B., et al. Dietary supplementation with *Artemisia argyi* extract on inflammatory mediators and antioxidant capacity in broilers challenged with lipopolysaccharide. *Italian Journal of Animal Science*, **2020**, 19: 1091–1098. https://doi.org/10.1080/1828051X.2020.1816506

[11] Zhang, L., Xing, Y., Shi, L., et al. The effects of dietary supplementation of *Artemisia argyi* polysaccharide on immune and antioxidative functions in broilers. *Journal of Applied Animal Research*, **2022**, 50: 587–597. https://doi.org/10.1080/09712119.2022.2119982

[12] Jin, M., Zhu, Y., Shao, D., et al. Effects of polysaccharide from mycelia of *Ganoderma lucidum* on intestinal barrier functions of rats. *International Journal of Biological Macromolecules*, **2017**, 94: 1–9. https://doi.org/10.1016/j.ijbiomac.2016.09.099

[13] Liu, L., Li, Y., He, Y., et al. *Enterococcus faecium* HDRsEf1 inhibits lipopolysaccharide-induced downregulation of zona occludens-1 expression via toll-like receptor 2/4-mediated c-Jun N-terminal kinase/activator protein-1 signalling pathways. *Journal of Applied Microbiology*, **2022**, 132: 605−617. https://doi.org/10.1111/jam.15167

[14] Bian, M., Wang, J., Wang, Y., et al. Chicory ameliorates hyperuricemia via modulating gut microbiota and alleviating LPS/TLR4 axis in quail. *Biomedicine & Pharmacotherapy*, **2020**, 131: 110719. https://doi.org/10.1016/j.biopha.2020.110719

[15] Lan, M. B., Zhang, Y. H., Zheng, Y., et al. Antioxidant and immunomodulatory activities of polysaccharides from moxa (*Artemisia argyi*) leaf. *Food Science and Biotechnology*, **2010**, 19: 1463–1469. https://doi.org/10.1007/s10068-010-0209-5

[16] Wang, Y. J., Chen, Y., Zhang, X. Y., et al. New insights in intestinal oxidative stress damage and the health intervention effects of nutrients: a review. *Journal of Functional Foods*, **2020**, 75: 104248. https://doi.org/10.1016/j.jff.2020.104248

[17] He, Y., Xu, M., Lu, S., et al. Seaweed polysaccharides treatment alleviates injury of inflammatory responses and gut barrier in LPS-induced mice. *Microbial Pathogenesis*, **2023**, 180: 106159. https://doi.org/10.1016/j.micpath.2023.106159

[18] Li, R. L., Zhao, D. Y., Li, P. P., et al. Effects of thymol and rosmarinic acid combination on growth performance, inflammatory response and intestinal health of lipopolysaccharide challenged rats. *Chinese Journal of Animal Nutrition*, **2022**, 34: 2009–2022. https://doi.org/10.3969/j.issn.1006-267x.2022.03.059

[19] Yin, L., Zhou, J., Chen, D., et al. A review of the application of near-infrared spectroscopy to rare traditional Chinese medicine. *Spectrochimica Acta Part A: Molecular and Biomolecular Spectroscopy*, **2019**, 221: 117208. https://doi.org/10.1016/j.saa.2019.117208

[20] Košťálová, Z., Hromádková, Z., Ebringerová, A. Structural diversity of pectins isolated from the styrian oil-pumpkin (*Cucurbita pepo* var. *styriaca*) fruit. *Carbohydrate Polymers*, **2013**, 93: 163–171. https://doi.org/10.1016/j.carbpol.2012.05.017

[21] Ji, X., Liu, F., Peng, Q., et al. Purification, structural characterization, and hypolipidemic effects of a neutral polysaccharide from *Ziziphus Jujuba* cv. Muzao. *Food Chemistry*, **2018**, 245: 1124–1130. https://doi.org/10.1016/j.foodchem.2017.11.058

[22] Geng, L., Hu, W., Liu, Y., et al. A heteropolysaccharide from *Saccharina japonica* with immunomodulatory effect on RAW 264.7 cells. *Carbohydrate Polymers*, **2018**, 201: 557–565. https://doi.org/10.1016/j.carbpol.2018.08.096

[23] Saia, R. S., Ribeiro, A. B., Giusti H. Cholecystokinin modulates the mucosal inflammatory response and prevents the lipopolysaccharide-induced intestinal epithelial barrier dysfunction. *Shock*, **2020**, 53: 242–251. https://doi.org/10.1097/SHK.0000000000001355

[24] Luo, J. Y., Li, Y. H., Fang, B. B., et al. Gene rs28362491 ins/del variation is associated with higher susceptibility to myocardial infarction in a Chinese Han population. *Scientific Reports*, **2020**, 10: 19518. https://doi.org/10.1038/s41598-020-72877-9

[25] Koh, A., de Vadder, F., Kovatcheva-Datchary P., et al. From dietary fiber to host physiology: short-chain fatty acids as key bacterial metabolites. *Cell*, **2016**, 165: 1332–1345. https://doi.org/10.1016/j.cell.2016.05.041

[26] Li, X., Chen, S., Zhao, Z. T., et al. Effects of polysaccharides from Yingshan Yunwu tea on meat quality, immune status and intestinal microflora in chickens. *International Journal of Biological Macromolecules*, **2020**, 155: 61–70. https://doi.org/10.1016/j.

ijbiomac.2020.03.198
[27] Wang, Y., Song, X., Wang, Z., et al. Effects of pine pollen polysaccharides and sulfated polysaccharides on ulcerative colitis and gut flora in mice. *Polymers*, **2023**, 15: 1414. https://doi.org/10.3390/polym15061414
[28] Sanjeewa, K. K. A., Nagahawatta, D. P., Yang, H. W., et al. Octominin inhibits LPS-induced chemokine and pro-inflammatory cytokine secretion from RAW264.7 macrophages via blocking TLRs/NF-κB signal transduction. *Biomolecules*, **2020**, 10: 511. https://doi.org/10.3390/biom10040511
[29] Cui, Y., Qu, Y., Yin, K., et al. Selenomethionine ameliorates LPS-induced intestinal immune dysfunction in chicken jejunum. *Metallomics*, **2021**, 13: mfab003. https://doi.org/10.1093/mtomcs/mfab003
[30] Wu, Y. R., Kuang, G. Y., Lu, F. G., et al. Pathological relationship between intestinal flora and osteoarthritis and intervention mechanism of Chinese medicine. *Chinese Journal of Integrative Medicine*, **2019**, 25: 716–720. https://doi.org/10.1007/s11655-019-3224-2
[31] Li, S., Zhuge, A., Wang, K., et al. Ketogenic diet aggravates colitis, impairs intestinal barrier and alters gut microbiota and metabolism in DSS-induced mice. *Food & Function*, **2021**, 12: 10210–10225. https://doi.org/10.1039/d1fo02288a
[32] Kaminsky, L. W., Al-Sadi, R., Ma, T. Y. IL-1β and the intestinal epithelial tight junction barrier. *Frontiers in Immunology*, **2021**, 12: 767456. https://doi.org/10.3389/fimmu.2021.767456
[33] Chen, M., Xiao, D., Liu, W., et al. Intake of *Ganoderma lucidum* polysaccharides reverses the disturbed gut microbiota and metabolism in type 2 diabetic rats. *International Journal of Biological Macromolecules*, **2020**, 155: 890–902. https://doi.org/10.1016/j.ijbiomac.2019.11.047
[34] Yin, Z., Liang, Z., Li, C., et al. Immunomodulatory effects of polysaccharides from edible fungus: a review. *Food Science and Human Wellness*, **2021**, 10: 393–400. https://doi.org/10.1016/j.fshw.2021.04.001
[35] Niu, Y., Dong, J., Jiang, H., et al. Effects of polysaccharide from *Malus halliana* Koehne flowers in cyclophosphamide-induced immunosuppression and oxidative stress on mice. *Oxidative Medicine and Cellular Longevity*, **2020**, 2020: 1603735. https://doi.org/10.1155/2020/1603735
[36] Akdis, C. A. Does the epithelial barrier hypothesis explain the increase in allergy, autoimmunity and other chronic conditions? *Nature Reviews Immunology*, **2021**, 21: 739−751. https://doi.org/10.1038/s41577-021-00538-7
[37] Wang, J., Liang, Q., Zhao, Q., et al. The effect of microbial composition and proteomic on improvement of functional constipation by *Chrysanthemum morifolium* polysaccharide. *Food and Chemical Toxicology*, **2021**, 153: 112305. https://doi.org/10.1016/j.fct.2021.112305
[38] Lai, L., Chen, Y., Tian, X., et al. Artesunate alleviates hepatic fibrosis induced by multiple pathogenic factors and inflammation through the inhibition of LPS/TLR4/NF-κB signaling pathway in rats. *European Journal of Pharmacology*, **2015**, 765: 234–241. https://doi.org/10.1016/j.ejphar.2015.08.040
[39] Zheng, J., Ahmad, A. A., Yang, C., et al. Orally administered *Lactobacillus rhamnosus* CY12 alleviates DSS-induced colitis in mice by restoring the intestinal barrier and inhibiting the TLR4-MyD88-NF-κB pathway via intestinal microbiota modulation. *Journal of Agricultural and Food Chemistry*, **2024**, 72: 9102–9166. https://doi.org/10.1021/acs.jafc.3c07279
[40] Liu, C., Cheng, L., Ji, L., et al. Intestinal microbiota dysbiosis play a role in pathogenesis of patients with primary immune thrombocytopenia. *Thrombosis Research*, **2020**, 190: 11–19. https://doi.org/10.1016/j.thromres.2020.03.012
[41] Zhang, J., Zhong, Y., Wang, D., et al. Wallace melon juice fermented with Lactobacillus alleviates dextran sulfate sodium-induced ulcerative colitis in mice through modulating gut microbiota and the metabolism. *Journal of Food Science*, **2024**, 89: 2450–2464. https://doi.org/10.1111/1750-3841.16973